

Experimental Verification of the Nozzle Shape Optimization for Self-Field MPD Thruster

IEPC-2005-163

*Presented at the 29th International Electric Propulsion Conference, Princeton University
October 31 – November 4, 2005*

Daisuke Nakata*, Kyoichiro Toki†, Ikkoh Funaki‡
Yukio Shimizu§, Hitoshi Kuninaka¶, Yoshihiro Arakawa||

* || *University of Tokyo, 7-3-1, Hongo, Bunkyo-ku, Tokyo 113-8656, Japan*

† *Tokyo University of Agriculture and Technology,
2-24-16, Nakacho, Koganei-shi, Tokyo 184-8588, Japan*

‡ § ¶ *Japan Aerospace Exploration Agency
Institute of Space and Astronautical Science
3-1-1, Yoshinodai, Sagami-hara-shi, Kanagawa 229-8510, Japan*

Abstract: The performance of MagnetoPlasmaDynamic (MPD) thruster is strongly affected by its electrode nozzle geometries. A lot of analytical or experimental researches have been conducted, but general guidelines have not been obtained yet. Recently, Toki pointed out the existence of optimum electrode geometry by a numerical approach. The optimum geometry had a few characteristic features, but they were not confirmed experimentally. In this paper, considering such features, a series of systematic experiments were conducted. It was found that the throat diameter in converging-diverging configuration is very critical parameter whereas the exit diameter of Flared anode hardly affected the thruster performances.

Nomenclature

J	= Discharge Current, kA
V	= Discharge Voltage, V
T	= Thrust, N
\dot{m}	= Mass Flow Rate, g/s
P	= Input Power, kW
η	= Thrust Efficiency, %
r_c	= Cathode Diameter, mm
r_a	= Mean Diameter of Anode, mm
r_{in}	= Inlet Diameter of Anode, mm
r_{th}	= Throat Diameter of Anode, mm
r_{ex}	= Exit Diameter of Anode, mm

*Graduate Student, Department of Aeronautics and Astronautics, E-mail: nakata@ep.isas.jaxa.jp

†Professor, Department of Mechanical Systems Engineering, E-mail: toki@cc.tuat.ac.jp

‡Associate Professor, Space Transportation Division, E-mail: funaki@isas.jaxa.jp

§Research Engineer, Space Transportation Division, E-mail: shimizu@isas.jaxa.jp

¶Professor, Space Transportation Division, E-mail: kuninaka@isas.jaxa.jp

||Professor, Department of Aeronautics and Astronautics, E-mail: arakawa@al.t.u-tokyo.ac.jp

I. Introduction

NASA declared that they would pay primary attention to large-scale interplanetary missions using Nuclear Electric Propulsion (NEP)¹ after retirement of Space Shuttles. For such a NEP system, MagnetoPlasma-Dynamic (MPD) thruster will be a hopeful candidate in the future because of its very small specific weight ($<0.5\text{kg/kW}$)² and the reliability under the large input power ($>100\text{kW}$). In Addition, MPD thruster can use variety of gases or liquids as propellants.³

On the other hand, the most significant problem of MPD thruster is its quite low thrust efficiency. That discourages the motivation of practical use, therefore, other electric propulsion devices (Hall or Ion thrusters) are widely accepted now.⁴

To improve the efficiency, it is necessary to reduce the energy loss in the flow field. The fundamental principle of MPD thruster is to use the self-field Lorentz force for acceleration, so it is preferable to convert the input power into kinetic energy of working gas via electromagnetic force, not into heat energy. The most fundamental way to control the flow field is to arrange the electrode configuration. Applying the external magnetic field⁵ or changing the propellant injection patterns⁶ are also popular. But even considering the difference of the operating power range or operating condition (steady or pulsed), varieties of electrode nozzle configurations are adopted in each organization in the world⁷⁻⁹ (Fig.1).

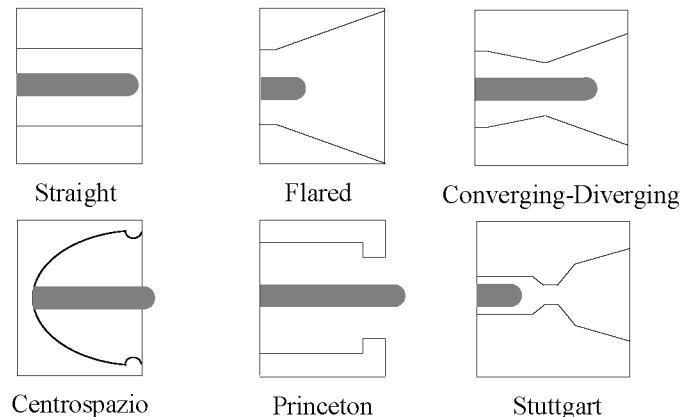


Figure 1. Various Electrode Geometries in the World

A series of experimental and analytical studies in Princeton University^{8,10,11} in the 1980s or the experimental works and numerical simulations in University of Stuttgart^{9,12,13} in the 1990s have brought sure-footed progress to this problem, but reliable optimum design method has not constructed yet. It can be said that the electrode configuration problem is still remaining.

II. Strategy and Objectives

When we consider how the optimum geometry should be under the fixed operational conditions, following the three pioneering works are thought to have the greatest generality. First work is Kunii's quasi one-dimensional analysis¹⁴ and experiments¹⁵. He analyzed five types of electrode geometries: Straight, Converging, Diverging (Flared), Converging-Diverging (C-D), and Diverging-Converging (D-C) and discussed which one was the best configuration. As an experimental result, simple Diverging geometry showed the best performance whereas Converging-Diverging type had been the best configuration in the analytical prediction. He concluded that some sort of neglected effects in his one-dimensional analysis (Hall effect or something) caused such a difference.

Second work is Martinez-Sanchez's study.¹⁶ He explained how the strong current concentration occurred in constant area geometry, and mentioned the limit of the efficiency;^a "the efficiency is no higher than

^aThis source is in his Space Propulsion Lecture Note of MIT, <http://ocw.mit.edu/OcwWeb/Aeronautics-and-Astronautics/16-522Spring2004/CourseHome/index.htm>

0.328 even if the voltage drops (near the electrode surface) could be eliminated. But this is intrinsic to the constant area geometry, and convergent-divergent geometry (Fig.2) can conceivably be exploited to improve efficiency.” And according to this suggestion, he obtained a current distribution pattern experimentally¹⁷ using his preferred configuration and confirmed that the current distribution became almost uniform in the channel. But the degree of performance improvement was not mentioned since any thrust measurement had not carried out.

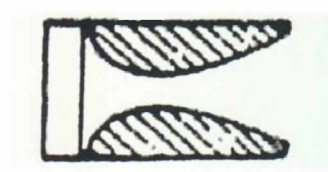


Figure 2. Preferred Anode Geometry Suggested by Martinez-Sanchez

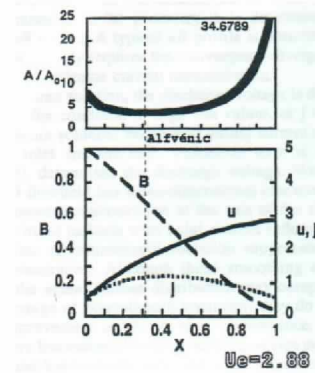


Figure 3. Toki's Optimum Geometry

Third work, which is directly connected to the current research, is Toki's numerical optimization.¹⁸ He led the optimum geometry (shown in Fig.3) using quasi-one dimensional framework under the condition in which pure electromagnetic force dominated the acceleration field. Resultant geometry was slowly converging in the upstream region and quickly diverging in the downstream. In the simulated flow field, this configuration made the moderately uniform current distribution over the entire channel and achieved an efficient acceleration of the propellant.

The physical backgrounds is as follows. As Martinez-Sanchez described, the discharge current tends to concentrate the root and the tip of the cathode in “Straight type” electrode. But the current distribution pattern should be moderately uniform along the axial direction of the channel since the local concentration of discharge current causes extreme joule heating and inefficient energy dissipation. In the case of electrothermal acceleration, this is acceptable if the heat energy is converted into the kinetic energy again, but if we want to use the electromagnetic force primarily, this is nothing but a waste. The rate of energy converted into the joule heat should be minimized. Therefore, converging-diverging geometry, which can drop the discharge current on the middle of the cathode and arrange the entire current distribution to be uniform, is preferable.

The underpinnings of Toki's optimum geometry has an great generality, but the resultant shape itself was led under very simple assumption: i.e., particle pressure, ionization, pumping force and electrical sheath were all ignored and electrical conductivity was set as a constant value, therefore, it might not be appropriate to apply this “optimum solution” to a real thruster directly. It has to be confirmed in the more precise simulation or direct experiment. The representative features of Toki's optimum geometry are as follows.

1. It has a throat to make discharge current uniform along the axial direction of the channel (not to accelerate the propellant into sonic speed.)
2. The throat is located at slightly upstream from the middle of the axis.
3. At the exit, electrode nozzle is widely diverging.

The purpose of this research is to verify whether these features are effective or not on improving the performance of real thruster. Besides, it is also important how the degree of improvement is. In Toki's calculation, it was anticipated that the “optimum” configuration would increase the efficiency by 1.25 times larger as that of the simple “Straight” geometry. But on this point, it is considered that the experimental result may be different because many effects were omitted in the simulation.

In these days, two or three-dimensional numerical code including various effect (for example, ionization, electrical or heat conductivity) has developed continuously in each organization in the world. Heiermann¹², Mikelides¹⁹, Sankaran²⁰, et al. In Japan, Funaki has constructed two-dimensional code to solve the internal MPD flow fields,²¹ and now, we try to develop more useful and precise one,²² and to couple the sophisticated optimum processes like a Genetic Algorithms into it.

To justify such a newly constructed numerical code, a series of experimental data are indispensable. Benchmark Thruster in Princeton University⁹ or DT thrusters in University of Stuttgart¹³ has played such a role, and in Japan, MY series in Osaka University²³ have been referred frequently. But when we try to discuss the geometry effect more detail, the experimental data sets of more various electrode configurations are required. Now, it is also expected that the experimental data in this report will be used as a database to give the validity into newly developed numerical simulation code.

III. Experimental Apparatus

A. Experimental Setup and Procedure

All experimental data in this paper were acquired with following procedure. Whole setup is shown in Fig.4. The MPD thruster is operated in a pulsed quasi-steady mode without applied magnetic field. Lorentz force is formed by the interaction between the discharge current and the self-induced magnetic field.

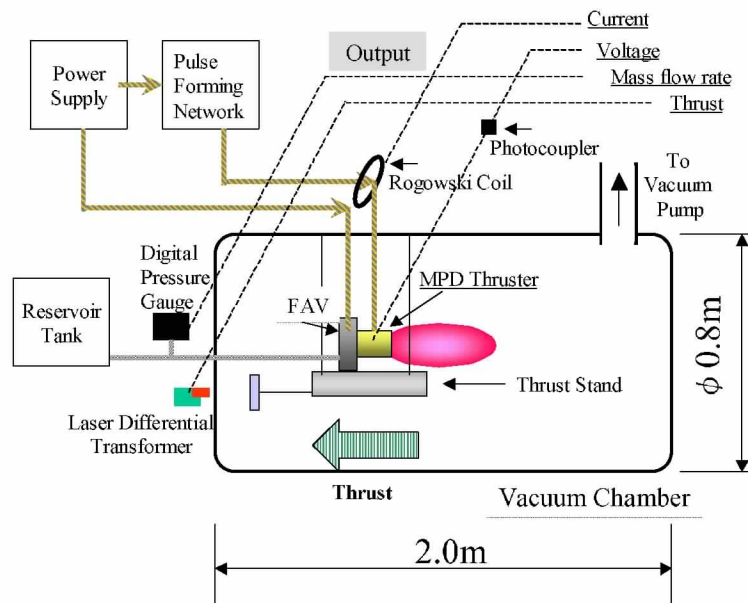


Figure 4. Experimental Setup

The stainless steel vacuum tank was 0.8m in diameter and 2.0m long, and its inner surface was completely covered by mylar sheet. The background pressure inside the tank was less than 10^{-2} Pa through the experiment. The power was supplied by a 2,000 μ F and 5kV capacitor bank constructing a pulse-forming network (PFN). Current monitoring was conducted by calibrated Rogowski coil and the discharge voltage was monitored via photo-coupler. Typical waveforms are shown in Fig.5 and Fig.6. Sampling frequency was 1MHz. The MPD thruster has no ignition plug, therefore initially applied high voltage induced the breakdown and then an arc discharge was initiated. The current pulse duration was about 0.5 ms. A Fast Acting Valve (FAV) provided gaseous propellant formed as a rectangular waveform lasting for 5ms. Pulsed mass flow rates were determined by the reduction of the reservoir pressure for each shot and it was divided by gas pulse duration. Shot-to-shot uncertainty was below 5%. Thrust measurement was conducted by the parallelo-pendulum method. The MPD thruster was suspended in a vacuum tank with two pairs of steel wires together with FAV. The amplitude of its swing determined the impulse. After subtracting the contribution of cold gas, it was transformed into net thrust when divided the quasi-steady duration. The

displacement of the thrust stand was measured by a laser position sensor. Whole thrust measurement system was calibrated by known impulse of steel ball impact. Typical impulse error was 0.4mNs at most. More detail information about the experiment system was described in Ref.24 or Ref.25.^b

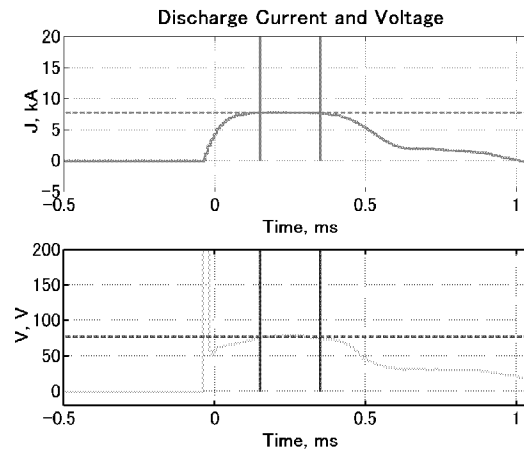


Figure 5. Typical Waveform of Discharge Current and Discharge Voltage (In the case of a stable operational condition: FL60-13, 2.4kA)

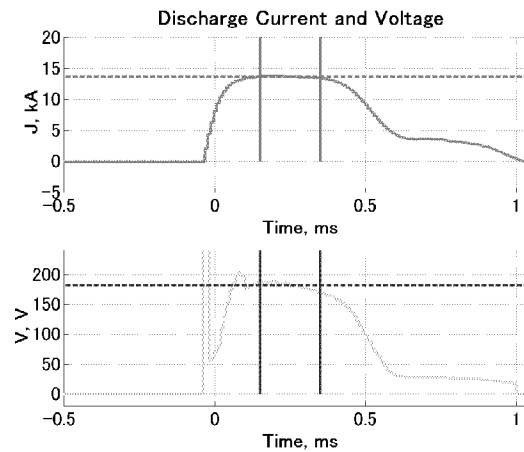


Figure 6. Typical Waveform of Discharge Current and Discharge Voltage (In the case of a unstable operational condition: FL60-13, 4.3kA)

B. Electrode Configurations

In this report, 9 types of configurations were prepared and they were labeled as follows.

FL60-13

Figure 7. the Shorthand of Electrode Geometry

In Fig.7, first two alphabets mean the fundamental classification. “ST” means “Straight” anode, “FL” means “Flared” anode, and “CD” means “Converging-Diverging (C-D)” anode. Each configurations have their derivations. (Straight configuration has no derivation.) Following number after two alphabets (e.g. FL“60”) indicates the representative scale parameter (in the case of Flared geometry, it means exit diameter, and in the case of C-D geometry, it means throat diameter.) The number after hyphen indicates cathode length. The unit of such numbers is “mm”. In this paper, only two cases; 13mm (short cathode) or 42mm

^bIn fact, these methods in Ref.24 and Ref.25 were not completely similar with present method, but almost same.

(long cathode) were used. Straight anode is always used with long cathode, Flared anode is used with short cathode, but C-D anode is used with both long or short cathode from time to time.

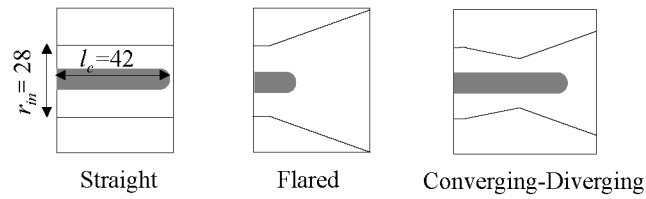


Figure 8. Fundamental classification of electrode configurations

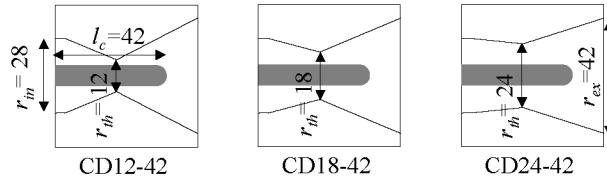


Figure 9. Converging-Diverging configurations with different throats

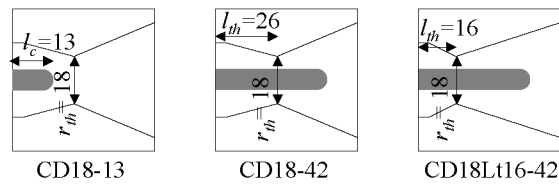


Figure 10. Converging-Diverging configurations with short cathode or a throat located at upstream

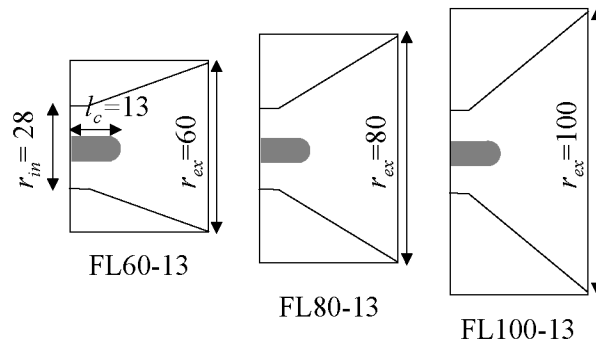


Figure 11. Flared configurations with different exit diameters

C. Operational Condition and Evaluation Policy

According to the Toki's assumption, this study aimed an operational range in which pure electromagnetic thrust component was dominant, i.e. electrothermal component could be neglected. When we compare the performances between two configurations, only such a operational range will be focused on. This region can be determined by the T/J^2 plot against J^2/\dot{m} . When T/J^2 curve converges into a constant value, it is considered that the electromagnetic force is sufficiently dominant. Figure 12 is the chart of T/J^2 plot against J^2/\dot{m} in the case of all configurations (9types) in this report. All plots are converging into a constant value in the region above $5 \times 10^{10} \text{ A}^2\text{s/kg}$.

From the above standpoint, argon was used as a propellant in all experiments. Three different mass flow rates (0.40g/s, 0.80g/s and 1.6g/s) were selected and experimented, but only the case of 0.80g/s will be reported in this paper because it was the most suitable case for comparison.

Onset condition is an important factor, but in this experiment, it was not examined in detail. One can know some sort of operation limit (but it was uncertain whether this means "onset" directly) from the length of voltage error bar in the current-voltage plot. If the error bar suddenly extends at certain point, that means discharge voltage waveform became instable at that point (Fig.6).

In the following section, we use the efficiency plot against "input power", instead of "specific impulse (I_{sp})". We regard a configuration which achieves high efficiency at lower power range as a better configuration, so the efficiency plot against "input power" is more useful for discussion. The I_{sp} is not obviously specified in this report, but it can be estimated easily from the thrust chart because all data in this report is acquired under the same mass flow rate (0.80g/s). 10N is corresponding to 1250s in I_{sp} .

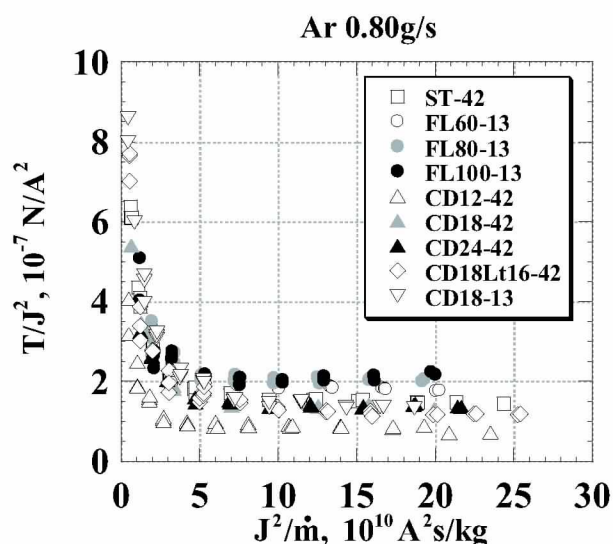


Figure 12. T/J^2 against J^2/\dot{m} characteristics of all configurations

IV. Experimental Results and Discussions

This section consists of following subsections. In each subsection, a few electrodes are collected into one group for a discussion.

1. Comparison between Straight, Flared and C-D geometry
2. The effect of throat diameter in C-D electrode configurations
3. The effect of the throat location in C-D electrode configurations
4. The effect of exit diameter in Flared electrode configurations

A. Comparison between Straight, Flared and C-D geometry

First of all, it must be confirmed whether CD geometry (with long cathode) is more efficient or not than any other typical configurations.

Figure 13 ~ 16 show the characteristics in the case of Straight, Flared and C-D (with long and short cathode) electrode configurations (they are shown in Fig.8). From Fig.16, it is recognized that CD18-42 shows the clear superiority in efficiency although the last 3 plots of CD18-42 were unfortunately in unstable condition. (One can know it from the length of voltage error bar shown in Fig.13.)

CD18-13, that is, the combination of CD anode and “short” cathode shows quite different performance compared to the case of CD18-42. It generated almost same thrust as the case of long cathode (Fig.14 or 15), but the voltage became much higher than that of CD18-42. The reason can be considered as follows; In the region below 8kA, it is considered that the distribution of discharge current was restricted in the upstream behind the throat, and then, the voltage curve became very flat. But in the region above 8kA, it was considered that the discharge current went over the throat and extended to downstream. Then, the current path became longer, and that led a rapid increase of the discharge voltage.

Flared configuration generated larger thrust compared to the case of Straight configuration, but there was no difference in efficiency because its voltage was also higher than that of Straight type.

Typically, the error bar becomes very long in efficiency plot, but it indicates conceivable “maximum” error, does not indicate the standard error.

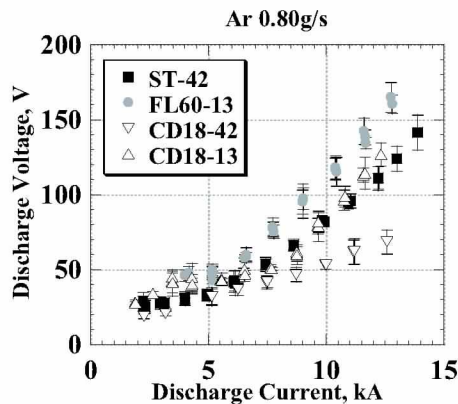


Figure 13. Discharge voltage against discharge current characteristics of representative electrode configurations

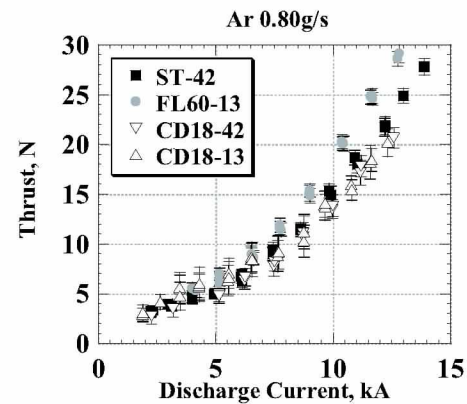


Figure 14. Thrust against discharge current characteristics of representative electrode configurations

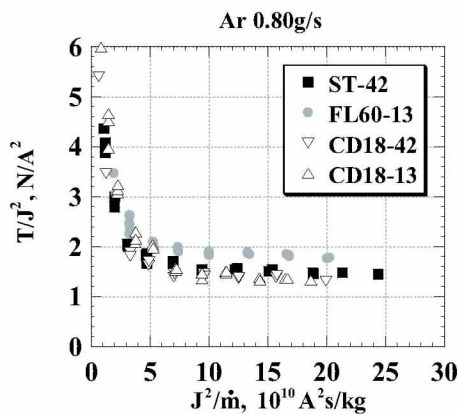


Figure 15. T/J^2 against J^2/\dot{m} characteristics of representative electrode configurations

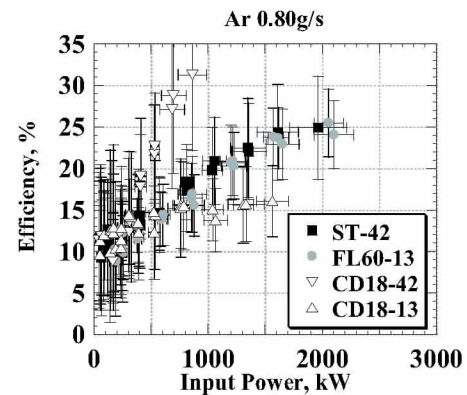


Figure 16. Propulsive efficiency against input power characteristics of representative electrode configurations

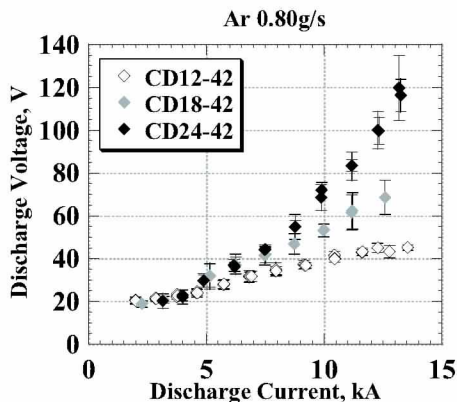


Figure 17. Discharge voltage against discharge current characteristics of 3 CD electrode configurations

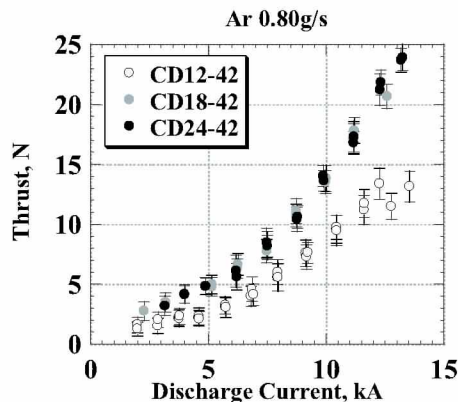


Figure 18. Thrust against discharge current characteristics of 3 CD electrode configurations

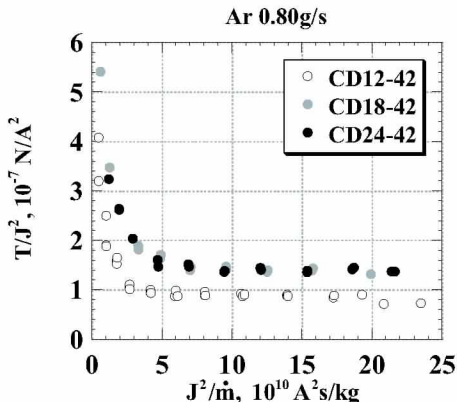


Figure 19. T/J^2 against J^2/m characteristics of 3 CD electrode configurations

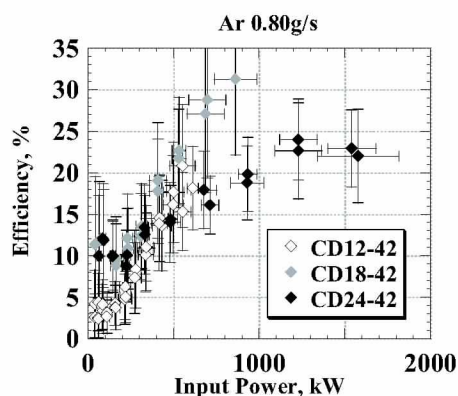


Figure 20. Propulsive efficiency against input power characteristics of 3 CD electrode configurations

B. The effect of throat diameter in C-D electrode configuration

In Kunii's study, contrary to the analytical expectation, Flared anode was more efficient than CD anode (with long cathode). He explained some sort of neglected effects in the one-dimensional analysis caused this discrepancy. It might be one of the conceivable reasons, but there was another significant problem. In his study, to begin with, the throat of CD anode used in the experiment was narrower than that used in the analysis. Although it was uncertain how much the difference of throat diameter affects the performance, but at least, each scale parameter had to be set equal between experiment and analysis. If CD configuration had a different throat diameter, the result might be different. In this study, it can be said that the comparison in the previous section was also rough because only one kind of configuration was used for ST, FL and CD as a representative. So, this point must be verified clearly.

In this section, three CD anodes with different throat diameters were prepared for comparison (they are shown in Fig.9). And the experimental results are shown in Fig.17~20.

First, apparent difference was recognized in the voltage characteristics (Fig.17). In the case of CD12-42, the discharge voltage was still 40V when the discharge current reached 10kA. Consequently, total input power became quite low. In this experiment, we can not obtain any data above 612kW in CD12-42 configuration because of the limit of ability of the capacitor.^c Judging from Fig.17, the voltage waveform did not become unstable even in 14kA.

In Fig.18 or Fig.19, CD18-42 and CD24-42 showed almost similar performance. Only CD12-42 generated smaller thrust. Resultantly, CD18-42 revealed the best efficiency among the three configurations. The

^cThis capacitor could not supply more than 15kA.

efficiency was 20% at 500kW, and reached 30% at 800kW, but a voltage hash was recognized at this point.

C. The effect of throat location in C-D electrode configuration

Not only the throat diameter but also its location of the axial direction should be taken into consideration. In Fig.3, we can see the throat part is located at slightly upper point from the middle of axis. From the point of physical meanings, since discharge current tends to concentrate more extremely into the tip of cathode rather than the root of the cathode, it is preferable to move the throat part into the upstream. Although Toki's optimization was conducted under very simple assumptions, this reason is quite acceptable even in real thruster.

In this verification, CD18-42 and "CD18Lt16", whose throat part was located at 1cm upstream position compared to that of CD18-42, were prepared (Fig.10).

The results are shown in Fig.21~24. The voltage of CD18Lt16-42 was slightly higher in the region below 5kA and above 10kA. The voltage instability emerged at almost same condition in both thrusters. The thrust curves had almost similar tendency between both configurations. Therefore, the difference of the voltage led the difference of the efficiency. And the result was opposite from the expectation; i.e. CD18Lt16 was inferior in the efficiency. It was considered that ignoring the ionization process in the calculation led the discrepancy. In a real thruster, some amount of energy is necessary to ionize the propellant in upstream region.

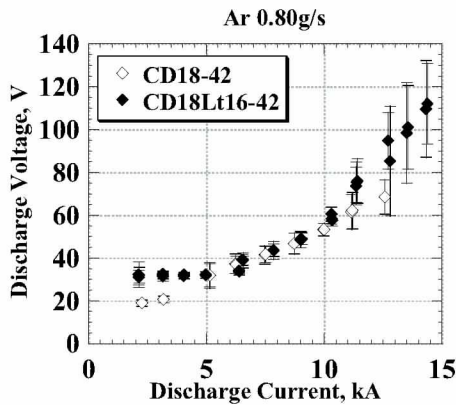


Figure 21. Discharge voltage against discharge current characteristics of 2 CD electrode configurations

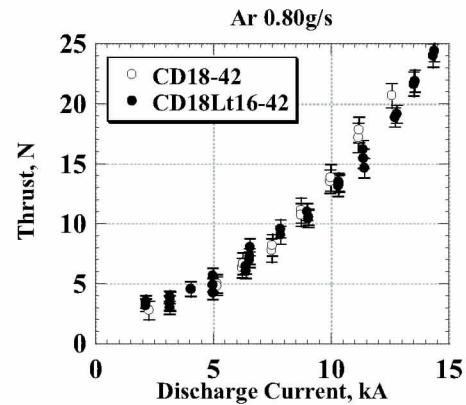


Figure 22. Thrust against discharge current characteristics of 2 CD electrode configurations

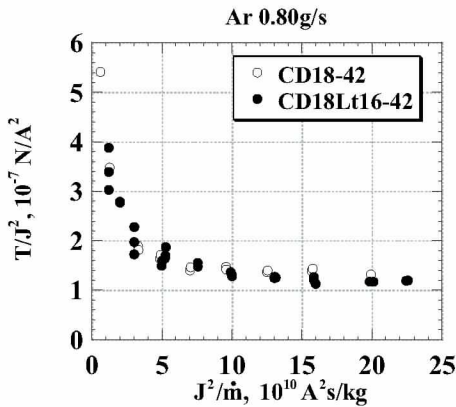


Figure 23. T/J^2 against J^2/m characteristics of 2 CD electrode configurations

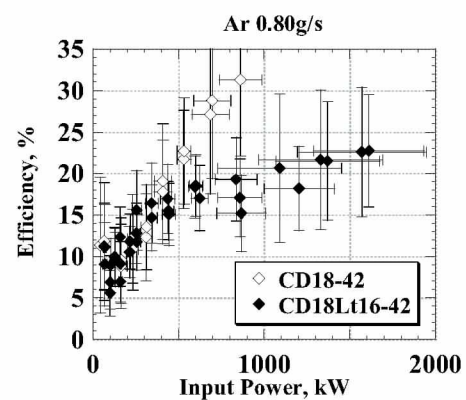


Figure 24. Propulsive efficiency against input power characteristics of 2 CD electrode configurations

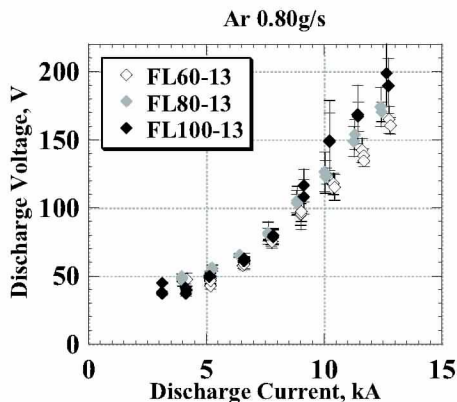


Figure 25. Discharge voltage against discharge current characteristics of 3 Flared electrode configurations

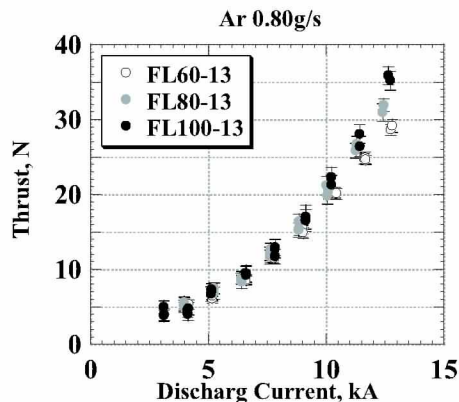


Figure 26. Thrust against discharge current characteristics of 3 Flared electrode configurations

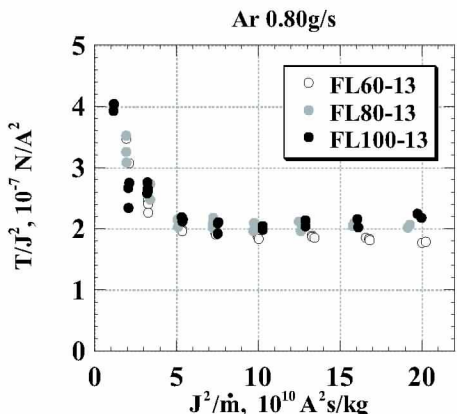


Figure 27. T/J^2 against J^2/\dot{m} characteristics of 3 Flared electrode configurations

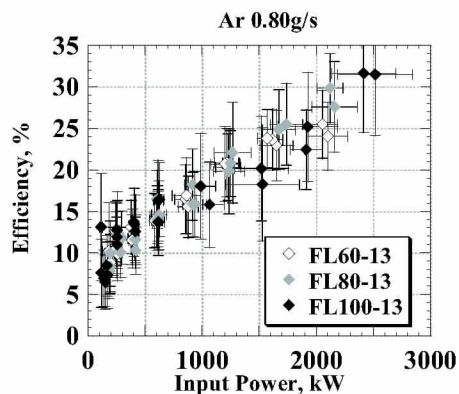


Figure 28. Propulsive efficiency against input power characteristics of 3 Flared electrode configurations

D. The effect of exit diameter in Flared electrode configuration

As one of the remarkable characteristics of Toki's optimum configuration (Fig.3), the widely divergent nozzle exit was recognized. According to Colasurdo,²⁶ this result was just caused by the ambiguity of end condition concerning the magnetic flux density in computation. Therefore, this tendency may not yield any improvement for the actual thruster.

But on the other hand, it is well known fact that the diverging nozzle makes assured improvement. At least, it leads large exhaust velocity and generates large thrust. These effect is caused by its large r_a/r_c ratio, but it is uncertain to what extent the enlargement of r_a/r_c is effective. In the past research, A. C. Malliaris²⁷ reported about the effect of r_a/r_c changing it from 2 to 8, but it was not the case of Flared configuration.

In this study, 3 Flared electrodes were prepared. Their overview and each scale parameter were shown in Fig.11. Resultant diverging angles were 22, 34, and 43 degree for FL60-13, FL80-13 and FL100. All of them were used with short cathode, considered as a forefront part of C-D configurations.

Experimental results are shown in Fig.25~28. Remarkable difference was not recognized between 3 configurations below 10 kA. In the region above 10kA, FL100-13 showed slightly larger thrust than the others. Besides, the voltage was also higher than the others and became unstable.

Although there was a few trivial difference, whole tendency between 3 geometries were quite similar. The reason is simple. Even if we use a widely enlarged anode, the discharge current did not extend into downstream. In the experiment, it was easily observed that the generated plasma was restricted in upstream. Besides, by a lack of propellant at the exit, the operation limit easily came in large current region.

Resultantly, the enlargement of exit diameter of Flared nozzle hardly affected the performance. If we change the propellant injection pattern more properly, some effect for the enlargement of nozzles may be recognized.

V. Discussions

Through the all experiments, it became clear that the CD18-42 was undoubtedly the best configuration. Besides CD12-42 seemed to be promising configuration could reach $\eta=30\%$ without any instability.

In Toki's calculation, it was anticipated that the "optimum" configuration would increase the efficiency by 1.25 times of the simple "Straight" geometry. If we adopted this conclusion directly into the experimental data, the upper limit $\eta=25\%$ in the case of Straight configuration should be improved into $\eta=31.25\%$ in the case of the optimum configuration. According to this viewpoint, remaining room for improvement seems to be little. But this was only an assumption under a simple quasi-one dimensional framework, and whether more efficient case exists or not is uncertain.

In this research or original Toki's analysis, only the configurations whose inner surface was "whole conductive anode" were intended. No configurations in which the part of the inner surface was covered by "insulator" was considered. Therefore, a lip anode configuration that has insulator part in its inner surface is outside of this study. Such a configuration is widely used in the world as represented by Princeton Benchmark Thruster (Fig.1), and its performance is typically good. According to the Ref.8, originally Ref.11, reported maximum efficiency of Benchmark thruster (in the case of argon propellant) was 30% at $P=3.8\text{MW}$ and $\dot{m}=6\text{g/s}$. Recently, more improved version was constructed and tested by Michael LaPointe in GRC^{28,29} and its maximum efficiency was reported as 35% at $P=2.8\text{MW}$ and $\dot{m}=0.5\text{g/s}$. So, it is necessary to include such types into optimization process hereafter.

The CD18-42 and the Princeton Benchmark Thruster seems to be quite different configurations, but they have great similarity in a certain point. The effect of CD anode with long cathode was to drop the discharge current on the middle region of the cathode and to avoid the current concentration into the edge. And Princeton Benchmark Thruster also enables that because of its uniquely protruding cathode.

The advantage of CD configuration is not only its conclusive high efficiency but also its low input power operation. CD18-42 can work by self-field electromagnetic force as a dominant thrust component even in multi-hundred kW range.

In this operation range, the DT2 (or DT7 or HAT) thruster in University of Stuttgart is undoubtedly the most superior. It recorded 27% at only $P=330\text{kW}$ in steady state operation.¹³ Generally, pulsed operation is disadvantageous because its cathode is always "cold condition" and slightly higher voltage is necessary compared to steady state operation. If CD18-42 is operated in steady state condition, the efficiency might become higher than now.

Our final goal is to achieve 40% in efficiency by changing the electrode configuration or using some cathode technique, not depending on particular propellant. Of course, from the viewpoint of pursuing high efficiency, lithium propellant is undoubtedly hopeful, but basic and continuous study of geometry optimization in simple self-field MPD thruster will be useful for all type of MPD thrusters for sure.

VI. Conclusion

The following conclusions were obtained in the present experiment.

- When we focused on the region in which the electromagnetic thrust component is dominant, Converging-Diverging anode with long cathode was the most superior electrode configuration. It enabled the efficient operation even in low input power range compared to the others.
- The characteristics of certain configuration should not be judged only from its representative configuration. The scale parameter of each part was important and must be taken into consideration. Especially in CD configuration, throat diameter strongly affects its performance.
- In the case of Flared anode, the effect of exit diameter (or diverging angle) was weak because the exhaust plume was detached from the anode surface.
- As for the problem of the throat location, CD18Lt16-42, whose throat part was located at upstream

compared to CD18-42, generated almost same thrust as that of CD18-42, but showed higher voltage. Therefore, resultant efficiency was poorer opposite to the analytical expectation.

- In Toki's analysis, even in the case of the optimum configuration, the efficiency was improved at most by 1.25 times compared to the simple Straight configuration. And in this experiment, through the all configurations, acquired maximum efficiency was about $\eta=31\%$. It was just 1.24 times larger than the case of Straight configuration.
- And then, all data obtained in this study is useful to verify newly constructed numeric codes as reference.

Acknowledgments

The author was supported through the 21st Century COE Program, "Mechanical Systems Innovation," by the Ministry of Education, Culture, Sports, Science and Technology in Japan.

References

- ¹M., SanSoucie, P. V., Hull, R. W., Irwin, M. L., Tinker, and B. W., Patton, "Trade Studies for a Manned High-Power Nuclear Electric Propulsion Vehicle," AIAA Paper 2005-2729, Jan., 2005.
- ²K., Sankaran, L., Cassady, A., D., Kodys, and E., Y., Choueiri, "A Survey of Propulsion Options for Cargo and Piloted Missions to Mars," *The Annals of the New York Academy of Science*, Vol. 1017, May, 2004, pp. 450-467.
- ³K., Uematsu, S., Morimoto, and K., Kuriki., "MPD Thruster Performance with Various Propellants," *Journal of Spacecraft and Rockets*, Vol. 22, No. 4, 1985, pp. 412-416.
- ⁴Steven, R., Oleson, and Frederick, W., Elliott, "The Electric Propulsion Segment of Prometheus 1," AIAA Paper 2005-3888, Jul., 2005.
- ⁵Y., Kagaya, H., Tahara, and T., Yoshikawa., "Effect of Applied Magnetic Nozzle in a Quasi-Steady MPD Thruster," IEPC Paper 03-031, Mar., 2003.
- ⁶K., Kuriki, M., Onishi, and S., Morimoto, "Thrust Measurements of KIII MPD Arcjet," *AIAA Journal*, Vol. 20, No. 10, Oct., 1982, pp. 1414-1419.
- ⁷M., Andrenutti, F., Paganucci, M., Frazzetta, G., and La Motta, and G., Schianchi, "Scale Effects on the Performance of MPD Thrusters," IEPC Paper 91-123, Oct., 1991.
- ⁸E., Y., Choueiri and J., K., Ziemer, "Quasi-Steady Magnetoplasmadynamic Thruster Performance Database," *Journal of Propulsion and Power*, Vol. 17, No. 5, 2001, pp. 967-976.
- ⁹Michael Winter, Monika Auweter-Kurtz, Christian Boie, Jorg Heiermann, and Helmut L., Kurtz, "Characterization of a Steady State MPD Thruster with Radiation Cooled Anode," IEPC Paper 99-167, Oct., 1999.
- ¹⁰D., Q., King, "Magnetoplasmadynamic Channel Flow for Design of Coaxial MPD Thrusters," Ph.D. Dissertation, Princeton University MAE Dept., 1981.
- ¹¹M., Wolff, A., J., Kelly, and R., G., Jahn, "A High Performance Magnetoplasmadynamic Thruster," IEPC Paper 84-32, Jul., 1984.
- ¹²Heiermann, J., Auweter-Kurtz, M., "Numerical and Experimental Investigation of the Current Distribution in Self-Field Magnetoplasmadynamic Thrusters," *Journal of Propulsion and Power*, Vol. 21, No. 1, 2005, pp. 119-127.
- ¹³T., Wegmann, Auweter-Kurtz, M., "Experimental Comparison of Steady State Nozzle Type and Cylindrical MPD Thrusters at High Current Levels," IEPC Paper 93-122, Sept., 1993.
- ¹⁴K., Kuriki, Y., Kunii, Y., Shimizu, "Idealized Model for Plasma Acceleration in an MHD Channel," *AIAA Journal*, Vol. 21, No. 3, 1983, pp. 322-326.
- ¹⁵Y., Kunii, Y., Shimizu, and K., Kuriki, "Current Distribution in a Quasi-Steady MPD Arcjet," AIAA Paper 82-1917, Nov., 1982.
- ¹⁶Martinez-Sanchez, M., "Structure of Self-Field Accelerated Plasma Flows," *Journal of Propulsion and Power*, Vol. 7, No.1, 1991, pp. 56-64.
- ¹⁷D., J., Heimerdinger, and M., Martinez-Sanchez, "Design and Performance of an Annular Magnetoplasmadynamic Thruster," *Journal of Propulsion and Power*, Vol. 7, No. 6, 1991, pp. 975-980.

- ¹⁸K., Toki, "Optimal Control of Quasi- One-Dimensional Self-Field Magnetoplasmdynamic Arcjet Flow-fields," *Journal of Propulsion and Power*, Vol. 13, No. 1, 1997, pp. 157-161.
- ¹⁹Mikellides, P. G., "Modeling and Analysis of a Megawatt-Class Magnetoplasmdynamic Thruster," *Journal of Propulsion and Power*, Vol. 20, No. 2, 2004, pp. 204-210.
- ²⁰Sankaran, K., Choueiri, E. Y., and Jardin, S. C., "Comparison of Simulated Magnetoplasmdynamic Thruster Flowfields to Experimental Measurements," *Journal of Propulsion and Power*, Vol. 21, No. 1, 2005, pp. 129-138
- ²¹Funaki, I., Toki, K., Kuriki, K., "Numerical Analysis of a Two-Dimensional Magnetoplasmdynamic Arcjet," *Journal of Propulsion and Power*, Vol. 13, No. 6, 1997, pp. 789-795.
- ²²Kubota, K., Funaki, I., and Okuno, Y., "Numerical Investigation of Ionization and Acceleration Processed in a Self-Field MPD Thruster," IEPC Paper 2005-089, Oct., 2005.
- ²³Tahara, H., Kagaya, Y., and Yoshikawa, T., "Quasi-Steady MPD Arcjets with Applied Magnetic Fields," AIAA Paper 85-2001, Jul., 1985.
- ²⁴Funaki, I., Toki, K., and Kuriki, K., "Electrode Configuration Effect on the Performance of a Two-Dimensional Magnetoplasmdynamic Arcjet," *Journal of Propulsion and Power*, Vol.14, No.6, Nov-Dec 1998, pp.1043-1048.
- ²⁵K., Kuriki, and H., Suzuki, "Transitional Behavior of MPD Arcjet Operation," *AIAA Journal*, Vol. 16, No. 10, Oct., 1978, pp. 1062-1067.
- ²⁶G., Colasurdo, and L., Casalino, "Channel Geometry for Optimal MPD Acceleration," AIAA Paper 2000-3540, 2000.
- ²⁷ A. C., Malliaris, R. R., John, R. L., Garrison, and D. R., Libby, "Performance of Quasi-Steady MPD Thrusters at High Powers," *AIAA Journal*, Vol. 10, No. 2, 1972, pp. 121, 122.
- ²⁸Michael R., LaPointe, "High Power MPD Thruster Development at the NASA Glenn Reserach Center," IEPC Paper 03-146, Mar., 2003.
- ²⁹Michael R., LaPointe, E., Strzempkowski, and E., Pencil, "High Power MPD Thruster Performance Measurements," AIAA Paper 2004-3467, Jul., 2004.